

# Sustainable Food Technology

Accepted Manuscript

This article can be cited before page numbers have been issued, to do this please use: N. Kanwal, M. Zhang, E. Bux and X. Wang, *Sustainable Food Technol.*, 2025, DOI: 10.1039/D5FB00839E.



This is an Accepted Manuscript, which has been through the Royal Society of Chemistry peer review process and has been accepted for publication.

Accepted Manuscripts are published online shortly after acceptance, before technical editing, formatting and proof reading. Using this free service, authors can make their results available to the community, in citable form, before we publish the edited article. We will replace this Accepted Manuscript with the edited and formatted Advance Article as soon as it is available.

You can find more information about Accepted Manuscripts in the [Information for Authors](#).

Please note that technical editing may introduce minor changes to the text and/or graphics, which may alter content. The journal's standard [Terms & Conditions](#) and the [Ethical guidelines](#) still apply. In no event shall the Royal Society of Chemistry be held responsible for any errors or omissions in this Accepted Manuscript or any consequences arising from the use of any information it contains.

## Sustainability Spotlight Statement

This research addresses the critical challenge of post-harvest food loss by introducing innovative, non-thermal pretreatments—sonication and pulsed electric field—to significantly reduce quality degradation and waste in apricots during high-temperature processing. By enhancing processing efficiency and extending shelf-life, this approach directly conserves resources, reduces energy consumption, and minimizes waste, contributing to a more resilient and sustainable food system.



1 **Mitigation of Apricot Quality Loss and Waste during High-Temperature**  
2 **Processing via Sonication and Pulsed Electric Field Pretreatments**

View Article Online

DOI: 10.1039/D5FB00839E

3  
4 **Nida Kanwal**<sup>1,2</sup>, **Min Zhang**<sup>1,3\*</sup>, **Erum Bux**<sup>4</sup>, **Wang Xiaojing**<sup>5</sup>

5  
6 <sup>1</sup> State Key Laboratory of Food Science and Resources, Jiangnan University, 214122

7 Wuxi, Jiangsu, China

8 <sup>2</sup> Jiangsu Province International Joint Laboratory on Fresh Food Smart Processing and  
9 Quality Monitoring, Jiangnan University, 214122 Wuxi, Jiangsu, China

10 <sup>3</sup> China General Chamber of Commerce Key Laboratory on Fresh Food Processing &  
11 Preservation, Jiangnan University, 214122 Wuxi, Jiangsu, China

12 <sup>4</sup> School of Biotechnology, Jiangnan University, Wuxi, China

13 <sup>5</sup> Haitong Food Group Company, Cixi, Zhejiang, China

14 \*Corresponding author: Professor Min Zhang, School of Food Science and  
15 Technology, Jiangnan University, 214122 Wuxi, Jiangsu Province, China

16 Tel.: 0086-510-85877225; Fax: 0086-(0)510-85807976

17 E-mail: [min@jiangnan.edu.cn](mailto:min@jiangnan.edu.cn)



18 **Abstract**

19 This study systematically evaluated the sequential application of 2% CaCl<sub>2</sub> soaking,  
20 sonication (150-300 W, 2-5 min), and pulsed electric field (PEF; 1.5-3.0 kV/cm, 30-  
21 90 min) pretreatments on firmness retention, weight loss, and bioactive compounds in  
22 apricot pieces prior to blanching at 85°C for 3 min, employing a response surface  
23 methodology (RSM) design encompassing 27 treatments (T1-T27) alongside controls  
24 (C1: blanching only; C2: CaCl<sub>2</sub> + sonication; C3: CaCl<sub>2</sub> + PEF). Conventional  
25 blanching (C1) reduced firmness to 0.23 N (baseline) and incurred 20% weight loss,  
26 while the optimized treatment T10 (200 W/3 min sonication + 1.5 kV/cm/30 min PEF)  
27 enhanced post-blanching firmness to 0.3335 N, achieving 45% retention ( $p < 0.05$  vs.  
28 C1; superior to C2: 20%, C3: 27%), and curtailed weight loss to 9% (55% reduction).  
29 Firmness peaked at moderate sonication/PEF intensities but declined under extremes  
30 due to over-permeabilization, with RSM plots revealing significant quadratic  
31 interactions ( $r = 0.92$  firmness-weight loss). Bioactive retention in T10 surpassed C1,  
32 yielding total polyphenol content (TPC) of  $14.9 \pm 0.8$  mg GAE/g DW (19% higher),  
33 total flavonoid content (TFC) of  $6.6 \pm 0.4$  mg CE/g DW (25% higher), DPPH  
34 scavenging of  $54 \pm 4.0\%$  (20% higher), and total anthocyanin content (TAC) of  $3.4 \pm$   
35  $0.2$  mg C3G/g DW (36% higher; ANOVA, Tukey's HSD,  $p < 0.05$ ), outperforming  
36 single pretreatments and correlating strongly with firmness ( $r = 0.88$  TPC-firmness).  
37 Fourier-transform infrared spectroscopy (FTIR) confirmed intensified pectin cross-  
38 linking ( $1730, 1620$  cm<sup>-1</sup>) and preserved glycosidic bonds in T10. The enhanced  
39 textural stability in T10 was further attributed to PME mediated demethylation of  
40 pectin, facilitating Ca<sup>2+</sup>-pectin cross-linking and strengthening the middle lamella  
41 structure, while X-ray diffraction (XRD) indicated elevated relative crystallinity (28.2%  
42 vs. 19.1% in C1), underpinning synergistic Ca<sup>2+</sup>-mediated pectin stabilization,



43 cavitation enhanced impregnation, and electroporation driven uniformity against  
44 thermal degradation. These findings demonstrate combined pretreatments as a viable  
45 strategy to mitigate blanching-induced quality loss in apricot pieces, enhancing  
46 process yield, texture, and nutritional value for sustainable stone fruit processing.  
47 **Key words:** Apricot blanching, Sonication, PEF, Firmness retention, Bioactive  
48 retention

View Article Online  
DOI:10.1039/D5FB00839E



## 49 1.Introduction

50 High temperature processing such as blanching is indispensable in apricot  
51 preservation chains but simultaneously drives substantial quality loss and economic  
52 waste. Blanching inactivates enzymes and reduces microbial load, yet the associated  
53 thermal load accelerates softening, tissue disintegration, drip loss, and degradation of  
54 color and bioactive compounds, ultimately diminishing product yield and nutritional  
55 and sensory value<sup>2</sup>. In the apricot industry, this over softening translates directly into  
56 flesh loss during subsequent handling and cutting, with weight losses on the order of  
57 20% representing a major bottleneck for process efficiency and sustainability<sup>3</sup>. At the  
58 same time, consumers increasingly demand minimally processed apricot products  
59 with fresh like texture and high retention of polyphenols, flavonoids, anthocyanins,  
60 and antioxidant activity, creating a pressing need for technologies that decouple  
61 enzyme inactivation from severe structural and nutritional damage<sup>1,4</sup>.

62 Apricot (*Prunus armeniaca L.*) is particularly sensitive to thermal treatments  
63 due to its delicate parenchyma tissue and high content of thermo labile bioactives  
64 such as carotenoids, phenolics, and vitamin C<sup>5</sup>. Conventional hot water or hot air  
65 blanching can cause rapid cell wall breakdown, pectin depolymerization, and loss of  
66 middle lamella integrity<sup>6</sup>, resulting in a marked decrease in firmness and pronounced  
67 shrinkage and drip loss. In apricot pieces and other stone fruits, increasing processing  
68 temperature and time has been associated with color deterioration, shrinkage, and  
69 progressive degradation of phenolic compounds and ascorbic acid, even when  
70 enzymatic inactivation is achieved<sup>7</sup>. These structural and compositional changes not  
71 only compromise texture and appearance but also reduce functional value, limiting the  
72 potential of apricot based products in health oriented markets<sup>8</sup>. Despite numerous  
73 process innovations, high temperature blanching remains one of the least optimized



74 steps regarding the simultaneous control of firmness, flesh yield, and nutrient  
75 retention. To mitigate heat induced quality damage, recent research has explored a  
76 range of physical pretreatments such as sonication, pulsed electric fields (PEF) <sup>9</sup>, and  
77 advanced blanching methods as tools to tailor tissue microstructure prior to high  
78 temperature exposure. Sonication can generate cavitation, micro-streaming, and  
79 mechanical stresses that modify cell walls and membranes, promote mass transfer,  
80 and, when properly controlled, enhance drying and improve rehydration while  
81 preserving color and bioactive compounds in various fruits <sup>10</sup>. For example,  
82 sonication-assisted osmotic dehydration has been shown to enhance antioxidant  
83 retention, maintain brighter color, and reduce shrinkage in litchi, plums, and other  
84 fruits, reflecting a more open and yet structurally resilient microstructure. However,  
85 excessive sonication intensity or exposure can lead to cell rupture and undesirable  
86 softening, and most studies have focused on drying rather than on optimizing firmness  
87 retention across a subsequent blanching step <sup>11</sup>.

88 PEF has emerged as another promising non-thermal or mild-thermal  
89 technology that uses short, high voltage pulses to induce electroporation of plant cell  
90 membranes <sup>11</sup>. In fruits such as tomatoes, kiwifruit <sup>12</sup>, and mango, PEF pretreatment  
91 has improved peeling efficiency and reduced peeling losses while maintaining or even  
92 enhancing textural and nutritional quality relative to conventional blanching or  
93 chemical peeling <sup>13</sup>. PEF has also been widely reported to increase the apparent  
94 extractability and measured content of phenolic compounds and anthocyanins, largely  
95 by facilitating diffusion from disrupted cell compartments into surrounding matrices.  
96 Nonetheless, most PEF studies have targeted processing endpoints such as peeling <sup>13</sup>,  
97 juice or polyphenol extraction, or drying kinetics, rather than the controlled

View Article Online  
DOI: 10.1039/D5FB00839E



98 preservation of fruit flesh integrity and firmness during high-temperature blanching of  
99 fresh like pieces <sup>12</sup>.

100 In parallel, calcium salt pretreatments especially CaCl<sub>2</sub> solutions have long  
101 been exploited to strengthen plant tissue by promoting pectin cross-linking within the  
102 cell wall matrix <sup>14</sup>. Calcium ions can interact with free carboxyl groups of  
103 homogalacturonan chains to form “egg-box” structures, thereby increasing pectin  
104 rigidity, reducing solubilization during heating, and improving firmness retention in  
105 blanched fruits and vegetables. Endogenous pectin methylesterase (PME) contributes  
106 to this reinforcement by catalyzing the demethylesterification of homogalacturonan  
107 domains <sup>15</sup>, increasing the density of Ca<sup>2+</sup>-accessible carboxyl groups and thereby  
108 promoting more extensive pectate network cross-linking during thermal  
109 processing. Yet, calcium treatments alone often fail to fully counteract the disruptive  
110 effects of prolonged heating and associated acid or enzyme catalyzed pectin  
111 depolymerization, particularly in soft fruits such as apricot <sup>16</sup>. Moreover, the  
112 interaction between Ca-mediated tissue stabilization and emerging physical  
113 pretreatments such as sonication and PEF has not been systematically characterized  
114 for stone fruits undergoing industrially relevant blanching conditions. Taken together,  
115 the literature highlights three critical gaps that constrain the development of robust,  
116 high quality apricot processing chains. First, while numerous studies have evaluated  
117 the impact of drying methods, storage conditions, or single pretreatments on apricot  
118 quality, there is a lack of integrative work that explicitly targets blanching-induced  
119 over softening and associated flesh loss in fresh like apricot pieces. Second, most  
120 investigations examine sonication, PEF, or CaCl<sub>2</sub> pretreatments in isolation, making it  
121 difficult to understand potential synergistic or antagonistic effects when these  
122 technologies are combined and sequentially applied prior to high-temperature



123 processing. Third, despite frequent reporting of color and global antioxidant metrics,  
124 limited attention has been paid to quantitative relationships between pretreatment  
125 conditions, firmness retention and flesh yield, and specific nutritional markers such as  
126 total polyphenols, flavonoids, and anthocyanins after blanching. As a result,  
127 processing decisions are often guided by qualitative observations rather than by  
128 optimized, mechanistically informed treatment combinations that jointly minimize  
129 waste and preserve nutritional and textural quality.

130 Although the above technologies have each shown promise in other fruits, their  
131 combined and mechanistically guided application to apricot remains largely  
132 unexplored. Unlike many fruits, apricot tissue exhibits high pectin solubility and rapid  
133 thermo softening even under mild heat, making it an excellent model to study the  
134 interplay between calcium mediated reinforcement and physical membrane disruption  
135 under combined pretreatments <sup>15, 17</sup>. Exploring the synergistic effects of sonication,  
136 PEF, and CaCl<sub>2</sub> in this context not only addresses an industrially relevant challenge  
137 flesh loss during blanching but also advances a mechanistic understanding that has not  
138 been established in previous fruit systems. The present study addresses these gaps by  
139 systematically investigating the mitigation of apricot quality loss and waste during  
140 high temperature blanching through the combined application of CaCl<sub>2</sub> soaking,  
141 sonication, and pulsed electric field pretreatments. A firm ripe apricot was selected  
142 and standardized by size, soluble solids, and maturity stage to minimize biological  
143 variability and enable robust comparisons among treatments. The process sequence  
144 CaCl<sub>2</sub> soaking, sonication in CaCl<sub>2</sub> solution, PEF application to apricot pieces,  
145 followed by blanching at 85 °C for 3 min was designed to emulate industrial  
146 blanching while allowing mechanistic interrogation of how each pretreatment step  
147 modulates tissue integrity and compound retention. By varying sonication power

View Article Online  
DOI: 10.1039/D5FB00839E



148 (150-300 W), sonication time (2-5 min), PEF intensity (1.5-3.0 kV/cm), and PEF  
149 duration (30-90 min) within a structured response surface methodology design, this  
150 work explores a broad processing space and identifies optimal combinations for  
151 concurrent physical and nutritional quality preservation.

152 This study innovates by explicitly quantifying firmness retention, flesh loss  
153 reduction, and detailed nutritional profiling relative to conventional blanching  
154 controls. The structured experimental design systematically evaluates pretreatment  
155 interactions across a broad processing space to identify optimal combinations that  
156 simultaneously enhance structural integrity and preserve bioactive compounds.  
157 Overall, this work contributes to the high impact literature on fruit processing by: (i)  
158 focusing on a thermally sensitive stone fruit and a technologically relevant  
159 high-temperature blanching step; (ii) systematically combining CaCl<sub>2</sub> soaking,  
160 sonication, and PEF into an integrated pretreatment strategy; (iii) quantifying their  
161 effects on firmness retention, flesh loss, and key nutritional and antioxidant markers  
162 following blanching; and (iv) identifying optimal pretreatment combinations that  
163 minimize waste while enhancing nutritional quality relative to conventional blanching.  
164 By clarifying the interplay between treatment intensity, exposure time, tissue integrity,  
165 and bioactive retention, the study offers actionable guidance for designing low-waste  
166 <sup>18</sup>, high-quality apricot processing operations and provides a transferable framework  
167 for applying combined non-thermal pretreatments to other heat sensitive fruits in  
168 modern food supply chains.

## 169 **2. Materials and methods**

### 170 **2.1 Sample Preparation**

171 Apricot (*Prunus armeniaca L.*) fruits <sup>19</sup>, Youyi cultivar, were procured from a  
172 local market in Wuxi, Jiangsu Province, China, affiliated with Jiangnan University.



173 Mature fruits of uniform size (approximately 40-50 mm equatorial diameter) and  
174 consistent ripeness (firm ripe stage, total soluble solids 12-15 °Brix) were selected to  
175 minimize variability in physicochemical properties across replicates. Post-  
176 procurement, fruits were immediately transported to the laboratory in insulated  
177 containers at  $4 \pm 1^\circ\text{C}$  and stored at  $2-4^\circ\text{C}$  with 85-90% relative humidity for up to 24  
178 h prior to processing, ensuring minimal physiological changes and microbial growth  
179 while maintaining firmness and quality. Fruits were thoroughly rinsed under running  
180 potable water to remove surface contaminants, followed by surface sterilization with  
181 0.1% (w/v) sodium hypochlorite for 1 min and two subsequent rinses with sterile  
182 distilled water. Pits were aseptically removed using a stainless steel knife. Fruit flesh  
183 was excised into pieces of  $2 \times 2 \times 2 \text{ cm}^3$  ( about 8 g per piece) with a Laboratory  
184 Manual Bench Cutting Knife (TOB New Energy, China) to ensure uniform geometry  
185 and reproducible surface area-to-volume ratio for treatment exposure. Prepared  
186 samples were randomly allocated into treatment groups ( $n = 12-15$  per group), each  
187 corresponding to a predefined combination of sonication power (W), PEF strength  
188 (kV/cm), and exposure duration (min), with untreated controls included for baseline  
189 comparison.

## 190 2.2 Methodology RSM design matrix

191 Apricot pieces were first soaked in 2%  $\text{CaCl}_2$  solution (at room temperature),  
192 then subjected to sonication in the same solution at specified power (150, 200, or 300  
193 W) and duration (2, 3, or 5 min). Post-sonication, pieces were removed from solution,  
194 cooled down, and subjected to PEF treatment (pieces only) at intensities of 1.5, 2.5, or  
195 3.0 kV/cm for 30, 60, or 90 min. Finally, samples underwent blanching at  $85^\circ\text{C}$  for 3  
196 min. Control (C1) received only blanching without pretreatments; C2 and C3 tested  
197 individual sonication or PEF effects, respectively. **Table 1** details the RSM<sup>20</sup> design



198 encompassing 27 combinatorial treatments (T1-T27) across sonication (150, 300 W View Article Online  
DOI: 10.1039/D5FB00839E  
2-5 min) and PEF (1.5-3.0 kV/cm, 30-90 min) parameters following 2% CaCl<sub>2</sub>  
200 soaking (25 ± 2°C for 10 minutes), plus controls C1-C3.

### 201 **2.3 Sonication pretreatment**

202 Sonication was performed using a lab-scale ultrasonic water bath (SK3300H,  
203 KUDOS Analytical Instrument Co., Ltd., Jiangsu, China; 20 kHz frequency; nominal  
204 powers of 150 W, 200 W, or 300 W) equipped with automatic temperature control  
205 and an inbuilt digital thermometer. Apricot pieces samples (about 100 g, 12-15 pieces  
206 per treatment) were processed via indirect contact immersion in the covered water  
207 bath container. Treatments T1-T9 received 150 W for 2 min each, T10-T18 received  
208 200 W for 3 min each, and T19-T27 received 300 W for 5 min each, with all 27  
209 treatments processed separately. The system maintained 25 ± 2°C throughout via  
210 integrated thermostat regulation. Post-sonication, samples were immediately cooled to  
211 4°C prior to subsequent PEF treatments.

### 212 **2.4 Pulsed electric field (PEF) pretreatment**

213 PEF pretreatment was carried out using a lab-scale PEF system comprising a  
214 high voltage pulse generator, capacitor bank, switching unit, and a customized  
215 treatment chamber designed for solid fruit pieces. Apricot pieces assigned to PEF  
216 treatments were positioned within the chamber in a non-immersed configuration,  
217 ensuring that samples were not in direct contact with the electrodes and were not  
218 suspended in a liquid medium, while maintaining a fixed parallel plate electrodes gap  
219 of 5 cm to achieve the desired electric field strengths. The applied electric field  
220 intensity was set at 1.5, 2.5, or 3.0 kV/cm, delivered as monopolar pulses with a pulse  
221 width of 50 µs and a pulse repetition frequency of 10 Hz, and the total treatment times  
222 were 30, 60, or 90 min depending on the experimental combination, corresponding to



223 a specific energy input of approximately 2.7 kJ/kg. These operating conditions fall  
224 within the range reported for moderate-intensity PEF treatments aimed at inducing  
225 reversible or limited irreversible electroporation in plant tissues while avoiding  
226 extensive structural destruction. The selection of field strength, pulse width,  
227 frequency, and treatment duration was guided by previous PEF studies on fruits and  
228 vegetables focused on texture preservation and mass transfer enhancement,  
229 complemented by preliminary trials on apricot that identified processing windows  
230 capable of enhancing firmness retention and reducing softening without causing  
231 visible burning, excessive tissue breakdown, or undesired heating. During treatment,  
232 voltage and current waveforms were periodically monitored using an oscilloscope and  
233 current probe to verify pulse stability and to calculate specific energy input, and the  
234 chamber temperature was kept below the threshold for noticeable thermal effects by  
235 intermittent operation and external cooling as needed. Extended 30-90 min exposures  
236 used cumulative low energy pulses (2.7kJ/kg total) for solid pieces diffusion (vs ms  
237 for liquids), with monitored waveforms confirming no electrolysis (no Cl<sub>2</sub> evolution),  
238 temperature rise less than 50°C via cooling and energy 10x lower than the high  
239 intensity PEF. Immediately after completion of PEF exposure under each condition,  
240 apricot samples were removed from the chamber and subjected to high temperature  
241 blanching.

## 242 **2.5 Blanching**

243 Blanching was performed using a controlled-temperature water bath system  
244 (KUDOS Analytical Instrument Co., Ltd., Jiangsu, China) equipped with an  
245 integrated thermostat, digital thermometer, and insulated cover to maintain precise  
246 heating and minimize evaporative losses. Pretreated apricot pieces (approximately  
247 100 g per batch, 12-15 pieces) were gently immersed in 300 mL of deionized water



248 (electrical conductivity  $< 1 \mu\text{S}/\text{cm}$ ) within heat-resistant borosilicate glass beakers  
249 (ratio of sample mass to water volume: 1:3), ensuring complete submersion without  
250 overcrowding to facilitate uniform heat penetration. The beakers were then placed in  
251 the preheated water bath, and the system temperature was rapidly stabilized at  $85 \pm$   
252  $1^\circ\text{C}$  under continuous stirring and monitoring, with blanching conducted for exactly 3  
253 min from the moment the sample core temperature reached  $85^\circ\text{C}$  (verified by  
254 inserting a fine tip thermocouple into representative pieces). This time-temperature  
255 combination was selected based on preliminary optimization trials and literature  
256 precedents for achieving peroxidase inactivation in stone fruits while limiting  
257 excessive softening and nutrient leaching. Upon completion, beakers were  
258 immediately transferred to an ice water bath ( $0\text{-}2^\circ\text{C}$ ) for rapid cooling to below  $10^\circ\text{C}$   
259 within 1 min, followed by gentle draining on sterile mesh screens to remove surface  
260 moisture without mechanical agitation. Treated samples were then patted dry with  
261 lint-free paper, weighed for yield calculations, and allocated for subsequent  
262 physicochemical analyses, with all operations replicated ( $n = 12\text{-}15$  per treatment  
263 group) under aseptic conditions to prevent microbial contamination.

## 264 2.6 Firmness Measurement

265 Firmness of blanched apricot pieces was determined using a TA.XTC texture  
266 analyzer (BosinTech, China) equipped with a 50 N load cell, following the  
267 standardized compression protocol described by Gull et al., 2021. Individual pieces  
268 were centrally positioned on the heavy duty test platform with the flattest face  
269 downward, and a cylindrical TA/2 probe (5 mm diameter) was applied  
270 perpendicularly to compress the sample to 30% strain. Instrument parameters were set  
271 as follows: trigger force of 3.0 g, pre-test speed of 2.0 mm/s, test speed of 1.0 mm/s,  
272 post-test speed of 2.0 mm/s, and a 10 s data acquisition interval to capture peak force



273 stability. Maximum compression force (N) was recorded as the firmness index<sup>21</sup> with  
 274 measurements performed in triplicate per sample (n = 12-15 per treatment group) at  
 275 ambient temperature (20 ± 2 °C) and relative humidity of 50-60%, ensuring minimal  
 276 dehydration between replicates. Firmness retention (%) was calculated relative to the  
 277 untreated blanched control (C1).

## 278 2.7 Weight Loss Measurement

279 Weight loss due to blanching-induced moisture evaporation and tissue  
 280 softening was quantified gravimetrically for each apricot sample using an analytical  
 281 balance (precision ± 0.001 g; Mettler Toledo, China) with reference to the protocol  
 282 outlined by Abidi et al., (2023)<sup>22</sup>. Uniform batches of pre-treated apricot pieces were  
 283 weighed immediately prior to immersion in the blanching setup, subjected to the full  
 284 pretreatment sequence (CaCl<sub>2</sub> soaking, sonication, PEF) followed by hot water  
 285 blanching at 85 °C for 3 min, and then rapidly cooled in an ice bath (0-2 °C) for 1 min,  
 286 surface-drained on sterile mesh sieves for 30 s, and gently patted dry with lint-free  
 287 absorbent paper to remove excess moisture without compressing the tissue. Final  
 288 mass (M<sub>f</sub>M<sub>f</sub>) was recorded within 2 min post-cooling to minimize post-blanching  
 289 evaporation artifacts. Absolute weight loss (WL, g) was calculated as WL=M<sub>0</sub>-  
 290 M<sub>f</sub>WL = M<sub>0</sub> - M<sub>f</sub>WL=M<sub>0</sub>-M<sub>f</sub>, and percentage weight loss (WL%) was determined  
 291 using Eq. (1):

$$292 \quad WL = ((M_0 - M_f) / M_0) \times 100 \quad \dots\dots(Eq. 1)$$

293 where M<sub>0</sub>M<sub>0</sub> is the initial mass before blanching and M<sub>f</sub>M<sub>f</sub> is the final mass  
 294 after blanching and cooling. Measurements were conducted in triplicate per treatment  
 295 group, with samples handled under controlled humidity (50-60% RH) at 20 ± 2 °C to  
 296 ensure reproducibility, enabling direct assessment of pretreatment efficacy in  
 297 mitigating blanching-associated food waste (FW).



## 298 **2.8 Extraction of polyphenolic compounds**

299 A 1 g sample of apricot tissue was placed into a 100 mL amber glass bottle.  
 300 To this, 50 mL of an 80% methanol solution, containing 0.1% hydrochloric acid, was  
 301 added. The mixture was stirred for 1 hour using a magnetic stirrer to ensure thorough  
 302 mixing. Afterward, the mixture was centrifuged at 4400 rpm for 10 minutes. This  
 303 extraction process was repeated three times, and the resulting supernatants were  
 304 combined. The pooled extract was concentrated to a final volume of 1 mL, transferred  
 305 to a graduated amber bottle, and diluted with 80% methanol to a total volume of 15  
 306 mL to prepare the test solution.

## 307 **2.9 Determination of total polyphenol content (TPC)**

308 TPC was quantified using the Folin-Ciocalteu colorimetric method as outlined  
 309 in previous studies by Raposo et al., 2024 with slight modifications<sup>23, 24</sup>. For this  
 310 assay, 25  $\mu$ L of the sample (both test and gallic acid standard solutions) were pipetted  
 311 into a 96-well microplate. Next, 125  $\mu$ L of 0.2 N Folin-Ciocalteu reagent was added  
 312 to each well, followed by shaking and allowing the reaction to proceed at room  
 313 temperature for 6 minutes. Subsequently, 100  $\mu$ L of 0.075 g/mL sodium carbonate  
 314 solution was added, mixed thoroughly, and incubated in the dark for 60 minutes. The  
 315 absorbance was measured at 765 nm. Gallic acid standard solutions of 0.01, 0.03, 0.06,  
 316 0.12, 0.2, 0.4, and 0.5 mg/mL were used to create a calibration curve. In cases where  
 317 the test sample concentration exceeded the standard range, the sample was  
 318 appropriately diluted before measurement. The TPC was expressed as milligrams of  
 319 gallic acid equivalents (GAE) per gram of dry weight (DW). All assays were  
 320 conducted in triplicate for each treatment to ensure consistency and accuracy of the  
 321 results.

$$322 \quad \text{TPC (mgGAE/gDW)} = \left( \frac{A_{\text{Sample}} - A_{\text{Blank}}}{A_{\text{Standard}}} \right) \times C_{\text{Standard}} \times \frac{V_{\text{total}}}{V_{\text{Sample}}} \times \frac{1}{m_{\text{sample}}}$$



323 Where:

View Article Online  
DOI: 10.1039/D5FB00839E

324  $A_{\text{sample}}$  = Absorbance of the sample,  $A_{\text{Blank}}$  = Absorbance of the blank,  $A_{\text{standard}}$  =  
325 Absorbance of the standard,  $C_{\text{standard}}$  = Concentration of the standard,  $V_{\text{total}}$  = total  
326 volume of the extract,  $V_{\text{sample}}$  = Volume of the sample used,  $m_{\text{sample}}$  = mass of the  
327 sample.

## 328 **2.10 Determination of total flavonoid content (TFC)**

329 The TFC content was measured using the sodium nitrite-aluminum chloride  
330 method, as described by Chen et al., 2021 with slight modifications<sup>25</sup>. To begin, 200  
331  $\mu\text{L}$  of the sample (both test and catechin standard solutions) was transferred into a 1.5  
332 mL centrifuge tube. Then, 550  $\mu\text{L}$  of a 5% sodium nitrite solution was added to the  
333 tube, and the mixture was vortexed and allowed to react for 5 minutes. After the  
334 reaction, 75  $\mu\text{L}$  of a 10% aluminum chloride solution was added, and the mixture was  
335 vortexed again, allowing the reaction to continue for an additional 6 minutes. Finally,  
336 500  $\mu\text{L}$  of 1 mol/L sodium hydroxide solution was introduced, and the mixture was  
337 vortexed once more. The absorbance of the resulting solution was measured at 510  
338 nm using a UV-Vis spectrophotometer. Catechin was used as the reference standard,  
339 and a calibration curve was prepared using catechin standards ranging from 0 to 100  
340  $\mu\text{g/mL}$ . The concentrations were prepared in the same solvent as the sample extracts.  
341 The total flavonoid content was calculated and expressed as milligrams of catechin  
342 equivalents per gram of dry weight (mgCE/gDW), with catechin serving as the  
343 reference compound for the calculation. This method was selected because catechin is  
344 commonly used for flavonoid quantification and facilitates comparison with other  
345 research studies.

346 Calculation of total flavonoid content (TFC):

$$347 \quad \text{TFC (mgCE/gDW)} = \left( \frac{A_{\text{Sample}} - A_{\text{Blank}}}{A_{\text{Standard}}} \right) \times C_{\text{Standard}} \times \frac{V_{\text{total}}}{V_{\text{Sample}}} \times \frac{1}{m_{\text{sample}}}$$



348 Where:

349  $A_{\text{sample}}$  = Absorbance of the sample,  $A_{\text{Blank}}$  = Absorbance of the blank,  $A_{\text{standard}}$  =  
 350 Absorbance of the standard,  $C_{\text{standard}}$  = Concentration of the standard,  $V_{\text{total}}$  = total  
 351 volume of the extract,  $V_{\text{sample}}$  = Volume of the sample used,  $m_{\text{sample}}$  = mass of the  
 352 sample

### 353 2.11 DPPH radical scavenging assay

354 Antioxidant activity was assessed in all treatment groups (control, pretreated)  
 355 using the DPPH (2,2-diphenyl-1-picrylhydrazyl) free radical scavenging method, as  
 356 described by Baba et al., (2024). The procedure followed the protocol outlined by  
 357 Brand Williams, Cuvelier, and Berset (1995). For each sample, 1 mg of dried extract  
 358 was mixed with 1 mL of a 100  $\mu\text{M}$  DPPH solution, prepared in 95% ethanol. The  
 359 mixture was thoroughly shaken and incubated at room temperature for 30 minutes.  
 360 Following the incubation, the absorbance of the solution was measured at 517 nm  
 361 using a UV-Vis spectrophotometer, as detailed in studies by Sanna et al., 2012<sup>26</sup> and  
 362 Dzięcioł et al., 2023<sup>27</sup>. The absorbance values were compared to a Trolox calibration  
 363 curve, which was prepared using Trolox solutions ranging from 10 to 100  $\mu\text{M}$ . The  
 364 linearity of the calibration curve was verified by plotting the absorbance of the Trolox  
 365 standards against their concentrations. The scavenging activity was determined by  
 366 comparing the sample absorbance to that of the Trolox standards. The results were  
 367 expressed as the percentage inhibition of DPPH radicals, allowing a comparison of  
 368 antioxidant activity across different pre-treatment groups. All measurements were  
 369 performed in triplicate, and data are presented as the mean  $\pm$  standard error (SE).

370 DPPH radical scavenging activity calculation:

$$371 \text{ DPPH Activity (\%)} = \left( \frac{A_{\text{control}} - A_{\text{sample}}}{A_{\text{control}}} \right) \times 100$$

372 Where:



373  $A_{\text{control}}$  = Absorbance of the DPPH control (without sample),  $A_{\text{sample}}$  = Absorbance  
 374 of the sample after reaction with DPPH.

### 375 **2.12 Determination of total anthocyanin content (TAC)**

376 The TAC was determined using the pH differential method, with slight  
 377 modifications, as described by Taghavi et. al., 2023<sup>28</sup> and Ziemlewska et. al., 2023<sup>29</sup>.  
 378 A 0.1 mL aliquot of the extract was added to a 5 mL brown centrifuge tube, followed  
 379 by the addition of 2.9 mL of a potassium chloride-hydrochloric acid buffer (pH 1.0),  
 380 and the mixture was thoroughly mixed. Next, 300  $\mu\text{L}$  of this solution was transferred  
 381 into a 96-well plate. A second aliquot of 0.1 mL of the extract was taken and placed  
 382 into another 5 mL brown centrifuge tube, to which 2.9 mL of sodium acetate buffer  
 383 (pH 4.5) was added and mixed. From this, 300  $\mu\text{L}$  was transferred to a second well of  
 384 the plate. The absorbance of both solutions was measured at 520 nm and 700 nm  
 385 using a multifunctional microplate reader.

386 The total anthocyanin content was calculated according to formula:

$$387 \quad \text{Total anthocyanin content (mgC3G/gDW)} = \frac{A_{\text{pH}1} - A_{\text{pH}4.5}}{\epsilon \times l \times m_{\text{sample}}} \times V_{\text{total}}$$

388  $A_{\text{pH}1}$  = Absorbance of the sample at pH 1.0,  $A_{\text{pH}4.5}$  = Absorbance of the sample at pH  
 389 4.5,  $V_{\text{total}}$  = total volume of the extract,  $\epsilon$  = molar extinction coefficient of cyanidin-3-  
 390 glucoside (in  $\text{L} \cdot \text{mol}^{-1} \cdot \text{cm}^{-1}$ ),  $l$  = Path length of the cuvette (cm),  $m_{\text{sample}}$  = Mass of  
 391 the sample (g).

### 392 **2.13 FTIR and XRD analysis**

393 To connect molecular and compositional changes with macroscopic texture,  
 394 this study employed FTIR, XRD, and TPA on freeze-dried apricot samples from  
 395 different pretreatments. To create a powdered form of apricot pieces, freeze-drying  
 396 was chosen as a sustainable method for quality preservation. The samples underwent  
 397 a series of ethanol dehydration steps (30%, 50%, 70%, 90%, and 100%) to effectively



398 remove moisture, as outlined by Li et. al., 2024. Prior to the dehydration process,  
399 glutaraldehyde (C<sub>5</sub>H<sub>8</sub>O<sub>2</sub>: MACKLIN, 2.5% in water, pH 7.2-7.4) was used as a  
400 fixative agent. Following dehydration, the samples were freeze-dried for 7 hours to  
401 facilitate precise and accurate analysis using FTIR, XRD techniques.

### 402 **2.13.1 Fourier Transform Infrared Spectroscopy (FTIR)**

403 The chemical structure was identified using an FT-IR spectrophotometer  
404 (Nicolet iS10, Thermo Fisher Scientific Co. Ltd., Waltham, Massachusetts, USA)  
405 following the method <sup>30</sup> outlined by Lin et al., 2019. In this process, the sample  
406 powder was mixed with KBr powder in a ceramic mortar, and the resulting mixture  
407 was pressed. The FT-IR spectra of the samples, spanning a wavelength range of 500-  
408 4000 cm<sup>-1</sup>, were recorded in transmission mode with a resolution of 4 cm<sup>-1</sup>.

### 409 **2.13.2 X-ray Diffraction (XRD)**

410 Crystallinity was evaluated using an X-ray diffractometer (D2PHASER,  
411 Bruker AXS Co. Ltd., Karlsruhe, Germany), with a scanning range of 5-80° for the  
412 diffraction angle (2θ). The X-ray diffraction patterns of the samples were analyzed  
413 using the MDI Jade 6 software as described by Mannana et.al., 2006 <sup>31</sup>.

414 The relative crystallinity (RC) was calculated using the following formula:

415 
$$RC (\%) = (\text{Sum of total crystalline peak areas}) / (\text{Sum of total crystalline and}$$
  
416 
$$\text{amorphous peak areas}) \times 100$$

### 417 **2.14 Statistical analysis**

418 All experiments were conducted in triplicate ( $n \geq 3$  independent replicates per  
419 treatment), and results are expressed as mean  $\pm$  standard deviation (SD). Data  
420 normality was verified using Shapiro-Wilk tests, followed by one-way analysis of  
421 variance (ANOVA) to assess differences among treatment groups, with post hoc  
422 pairwise comparisons performed via Tukey's honestly significant difference (HSD)



423 test significance determined at  $p < 0.05$ . Statistical computations were executed using  
424 IBM SPSS Statistics version 26.0 (IBM Corp., Armonk, NY, USA) for ANOVA and  
425 post hoc tests, and OriginPro 2025 (OriginLab Corp., Northampton, MA, USA) for  
426 graphical correlation matrices and response surface modeling.

### 427 **3. Results and Discussion**

#### 428 **3.1 Firmness retention**

429         Blanching at 85°C for 3 min without pretreatments (C1) reduced the  
430 maximum compression force of apricot pieces to 0.23 N, serving as the baseline for  
431 severe softening typical of thermal damage in stone fruits. In contrast, the optimized  
432 combined pretreatment T10 (2% CaCl<sub>2</sub> soaking, 200 W sonication for 3 min,  
433 followed by 1.5 kV/cm PEF for 30 min) markedly enhanced firmness to 0.3335 N,  
434 achieving 45% retention relative to C1, with statistical significance. Single  
435 pretreatments showed intermediate improvements: C2 (CaCl<sub>2</sub> + 200 W/3 min  
436 sonication, no PEF) reached 0.276 N (20% retention), while C3 (CaCl<sub>2</sub> + 1.5  
437 kV/cm/30 min PEF, no sonication) attained 0.2921 N (27% retention), underscoring  
438 the synergistic superiority of the full sequence over isolated technologies. Across the  
439 27-treatment RSM matrix, firmness trended upward with moderate sonication  
440 (peaking at 200 W/3 min across T10-T18, averaging 0.31 N or 35% retention) and  
441 low-moderate PEF (1.5-2.5 kV/cm/30-60 min yielding the highest values), but  
442 declined at extremes: low sonication (150 W/2 min, T1-T9: average 0.268 N, 16%  
443 retention) reflected insufficient microstructural modification, while high sonication  
444 (300 W/5 min, T19-T27: average 0.245 N, 6% retention) and prolonged PEF (e.g., 3.0  
445 kV/cm/90 min) caused over-permeabilization and cell disruption, as evidenced by  
446 response surface contour plots showing significant quadratic and interaction effects.  
447 These patterns align with the study's design to emulate industrial blanching while



448 optimizing sequential pretreatments, directly addressing the identified literature gap in  
449 integrated approaches for blanching-induced over-softening in apricot pieces. The  
450 superior firmness under T10 reflects  $\text{CaCl}_2$ -mediated cross-linking of pectin  
451 homogalacturonan chains into rigid 'egg-box' structures that resist thermal  
452 solubilization during blanching (**Fig.1**). Endogenous pectin methylesterase (PME)  
453 catalyzes demethylesterification of pectin methyl esters, exposing carboxyl groups for  
454  $\text{Ca}^{2+}$  chelation and forming stable pectate networks that preserve middle lamella  
455 integrity.

456 **Fig. 1** illustrates this PME- $\text{Ca}^{2+}$  mechanism, showing sequential  
457 demethylation followed by divalent cation bridging of homogalacturonan chains. This  
458 biochemical reinforcement, amplified by sonication enhanced  $\text{Ca}^{2+}$  impregnation and  
459 PEF-mediated solute distribution, underpins T10's 45% firmness retention. These  
460 firmness improvements are quantitatively depicted in **Figure 2a,b**, where T10 reached  
461 0.3335 N versus C1's 0.23 N baseline (45% retention;  $p < 0.05$ ), outperforming C2  
462 (0.276 N, 20%) and C3 (0.2921 N, 27%). The full RSM matrix (**Fig. 2b**) confirms  
463 peak firmness at moderate sonication/PEF conditions (T10-T18: 0.31 N), with  
464 quadratic declines at treatment extremes reflecting over-permeabilization effects. In  
465 apricots, with their delicate parenchyma and high pectin content, this stabilization is  
466 crucial against heat-induced protopectinase activation and  $\beta$ -eliminative degradation  
467 <sup>32</sup>, as seen in kiwifruit where  $\text{CaCl}_2$  pretreatments increased firmness by 30-50% post-  
468 heating by preserving cell-to-cell adhesion. Sonication at moderate intensity (200 W/3  
469 min) likely amplified this by generating cavitation bubbles and microstreaming that  
470 created transient microchannels (1-10  $\mu\text{m}$ ), enhancing  $\text{Ca}^{2+}$  diffusion into intercellular  
471 spaces without rupturing turgor-maintaining membranes, similar to sonication-  
472 assisted Ca impregnation in cherries that boosted firmness retention by 25% during



473 storage via improved ion permeation. Excessive sonication (300 W/5 min) in T19, T27  
474 however, induced excessive acoustic streaming and shear forces, leading to cell wall  
475 polysaccharides scission (FTIR: flattened 1050 cm C-O-C glycosidic) and excessive  
476 PME activation degrading protopectin to soluble fragments, confirmed by XRD  
477 amorphous halo expansion. Lower firmness (e.g., T27: 0.2346 N, only 2% retention),  
478 mirroring reports in strawberries where high-power sonication (>250 W) reduced  
479 texture by promoting pectin methyl esterase (PME) overactivity. Complementarily,  
480 PEF at 1.5 kV/cm/30 min (energy input 2.7 kJ/kg) induced reversible electroporation  
481 of tonoplast and plasma membranes, facilitating uniform solute exchange and heat  
482 penetration during blanching while minimizing localized overheating that exacerbates  
483 softening. This is consistent with PEF applications in potatoes and carrots <sup>33</sup>, where  
484 moderate fields (1-2 kV/cm) preserved hardness by limiting irreversible pore  
485 formation, unlike higher intensities (3 kV/cm) that dropped firmness by 20-30% due  
486 to cytoplasmic leakage. The synergy sonication priming tissue for deeper CaCl<sub>2</sub>  
487 action, PEF ensuring even distribution yielded T10's peak performance, exceeding  
488 individual effects. Further supporting this, the firmness gains correlate with  
489 anticipated microstructural preservation, where Ca-sonication-PEF reinforces the  
490 pectin-cellulose-hemicellulose matrix against blanching's hydrolytic assault, as will be  
491 detailed in subsequent FTIR and XRD analyses showing intensified carbonyl peaks  
492 and higher crystallinity in T10. Comparative studies in other soft fruits validate these  
493 mechanisms: in tomatoes, combined sonication and Ca pretreatments retained 40%  
494 more firmness post-blanching by synergizing cavitation-enhanced ion binding, while  
495 PEF-Ca sequences in mangoes improved texture by 35% via electroporation-aided  
496 cross-linking, preventing drip loss. In peaches, a close analog to apricots, stepwise  
497 blanching with CaCl<sub>2</sub> reduced softening by 28%, but adding sonication elevated it to

New Article Online  
DOI: 10.1039/D5FB00839E



498 45%, akin to our T10 results. Even in vegetables like green beans, PEF at 1.5 kV/cm  
499 preserved snap by 30% relative to hot water blanching, attributed to membrane  
500 stabilization that curtails enzyme diffusion. These parallels highlight the  
501 transferability of moderate-intensity pretreatments to thermo-labile tissues, where  
502 apricots' high water-soluble pectin makes them especially vulnerable, yet responsive  
503 to such interventions.

504 Technologically, T10's 45% firmness retention directly mitigates the 20%  
505 flesh loss in conventional apricot processing, as higher mechanical resilience (0.3335  
506 N vs. 0.23 N in C1) minimizes tissue disintegration during post-blanching handling,  
507 pitting, and slicing translating to a 55% waste reduction (from 20% to 9% weight loss,  
508 as quantified gravimetrically) and higher yields in industrial chains. This outperforms  
509 single methods (C2: 20%, C3: 27%) and aligns with sustainability goals, reducing  
510 economic losses estimated at 15-25% in stone fruit blanching lines. By decoupling  
511 enzyme inactivation from structural collapse, these findings offer a blueprint for  
512 minimally processed apricot products retaining fresh-like texture, fulfilling consumer  
513 demands while optimizing RSM-derived parameters for scalability.

### 514 **3.2 Weight loss reduction**

515 Hot water blanching at 85°C for 3 min without pretreatments (C1) induced  
516 substantial weight loss of 20% in apricot pieces (from initial 50 g to 40 g), primarily  
517 due to thermal softening, tissue disintegration, and drip loss from compromised cell  
518 walls and middle lamella. The optimized T10 pretreatment (2% CaCl<sub>2</sub> soaking, 200  
519 W sonication for 3 min, 1.5 kV/cm PEF for 30 min) dramatically mitigated this to 9%  
520 loss (final mass 45.5 g), representing a 55% reduction relative to C1, with highly  
521 significant differences. Single pretreatments yielded partial benefits: C2 (CaCl<sub>2</sub> +  
522 sonication) and C3 (CaCl<sub>2</sub> + PEF) both achieved approximately 12-15% loss,



523 highlighting the combined sequence's superior efficacy in preserving mass yield.  
524 Within the RSM matrix, weight loss minimized at moderate conditions (T10-T14: 8-  
525 11% loss), correlating strongly with firmness trends ( $r = 0.92$ ,  $p < 0.001$ ), but  
526 escalated under high sonication (T19-T27: 18-21%) or prolonged/intense PEF (e.g.,  
527 T12, T18: 13-15%), where excessive membrane disruption promoted moisture  
528 exudation. **Fig. 3** quantifies T10's 55% weight loss mitigation (9% vs. C1's 20%),  
529 with single pretreatments (C2/C3) at 12-15% confirming synergy. Optimal moderate  
530 conditions minimized loss to 8-11% (T10-T14), strongly correlating with firmness,  
531 while extremes exceeded 18% due to membrane rupture. Mechanistically, reduced  
532 loss stems from  $\text{CaCl}_2$ -reinforced pectin networks that seal intercellular spaces  
533 against blanching-induced syneresis, a core factor in stone fruits' high drip  
534 susceptibility. Sonication at optimal levels enhanced this by homogenizing  $\text{Ca}^{2+}$   
535 distribution via microchannels, preventing uneven weakening, while PEF's  
536 electroporation ensured rapid, uniform heat transfer to inactivate enzymes without  
537 prolonged exposure causing pectin hydrolysis. Extremes disrupted turgor balance,  
538 amplifying loss via osmotic gradients. This mirrors peaches, where Ca-sonication cut  
539 blanch loss by 50%, and tomatoes under PEF-Ca, retaining 40% more mass. T10's  
540 gains directly curb industrial flesh waste (20% to 9%), boosting yields and  
541 sustainability.

### 542 3.3 Bioactive retention

543 Blanching without pretreatments (C1) markedly diminished key bioactives in  
544 apricot pieces, yielding TPC of  $12.5 \pm 1.2$  mg GAE/g DW, TFC of  $5.3 \pm 0.5$  mg CE/g  
545 DW, TAC of  $2.5 \pm 0.3$  mg C3G/g DW, and DPPH radical scavenging activity of  $45 \pm$   
546  $3.2\%$ , reflecting thermal lability and leaching of thermo-sensitive phenolics from  
547 apricot's parenchyma. The optimized T10 condition elevated these metrics



548 substantially: TPC to  $14.9 \pm 0.8$  mg GAE/g DW (+19% vs. C1), TFC to  $6.6 \pm 0.4$  mg  
549 CE/g DW (+25%), TAC to  $3.4 \pm 0.2$  mg C3G/g DW (+36%), and DPPH to  $54 \pm 4.0\%$   
550 (+20%), all statistically superior. Single pretreatments lagged behind: C2 registered  
551 TPC  $13.1 \pm 1.3$ , TFC  $5.7 \pm 0.4$ , TAC  $2.8 \pm 0.3$ , DPPH  $50 \pm 3.5$  mg equivalents (%);  
552 C3 showed TPC  $14.2 \pm 1.4$ , TFC  $6.1 \pm 0.4$ , TAC  $3.2 \pm 0.4$ , DPPH  $52 \pm 4.1$  all  
553 intermediate, confirming synergistic enhancement from combined  $\text{CaCl}_2$ -sonication-  
554 PEF. Moderate pretreatments (e.g., T10-T14) maximizing retention via minimized  
555 leaching, while extremes (T19-T27) approximated C1 levels due to cell rupture  
556 facilitating solute efflux, as corroborated by strong correlations (TPC-firmness  $r =$   
557  $0.88$ ; DPPH-firmness  $r = 0.85$ ,  $p < 0.01$ ) and response surface models indicating  
558 interactive optima at 200 W/3 min sonication and 1.5 kV/cm/30 min PEF. These  
559 elevations arise from pretreatments curtailing blanching-induced degradation  
560 pathways,  $\text{CaCl}_2$  stabilizes vacuolar compartments housing phenolics<sup>34</sup>, shielding  
561 flavonoids and anthocyanins from heat/oxidative breakdown, akin to its role in  
562 strawberries preserving 25% more TPC post-processing via pectin-phenolic  
563 interactions. Moderate sonication promoted mild cavitation that enhanced  
564 extractability without rupture, increasing apparent bioactives by disrupting bound  
565 forms (e.g., cell wall phenolics), as observed in plums where sonication boosted  
566 flavonoid recovery by 20-30% during osmotic steps<sup>35</sup>. PEF's electroporation<sup>36</sup> at low  
567 intensity facilitated intra-tissue diffusion, homogenizing antioxidants and reducing  
568 localized thermal hotspots that degrade ascorbic acid-linked phenolics, paralleling  
569 mangoes where PEF-Ca retained 35% higher anthocyanins versus blanching alone.  
570 Synergy is evident: sonication preconditions for PEF-enhanced release<sup>37, 38</sup>, while Ca  
571 anchors released compounds against leaching, outperforming isolates as in kiwifruit  
572 dual pretreatments yielding 28% TPC gains. Excessive parameters, conversely,



573 permeabilized excessively, mimicking solvent extraction losses. **Fig. 4** (a-d) illustrates  
574 the superior retention of TPC (14.9 mg GAE/g DW), TFC (6.6 mg CE/g DW), TAC  
575 (3.4 mg C3G/g DW), and DPPH activity (54%) in T10-selected samples post-  
576 firmness screening, outperforming C1 (reductions of 19-36%) and single  
577 pretreatments (C2, C3), underscoring synergistic CaCl<sub>2</sub>-sonication-PEF protection  
578 against thermal leaching and degradation. These gains, linked to firmness-bioactive  
579 correlations ( $r=0.85-0.88$ ), arise from stabilized vacuolar phenolics and enhanced  
580 extractability without cell rupture, paralleling 20-40% improvements in plums,  
581 mangoes, and blueberries. Microstructural integrity in T10 (per XRD/FTIR) further  
582 validates this, positioning combined pretreatments as optimal for apricot bioactive  
583 preservation. Links to microstructure (detailed in FTIR/XRD) reveal preserved  
584 phenolic-carbohydrate matrices in T10, with reduced amorphous disruption  
585 correlating to bioactives. Comparatively, in blueberries, sonication-PEF cut bioactive  
586 loss about 40% post drying; cranberries showed Ca-sonication preserving flavonoids  
587 akin to apricots<sup>39,40</sup>.

### 588 3.4 FTIR Analysis

589 FTIR spectra from selected treatments (T10, C1, C2, C3) revealed distinct  
590 molecular fingerprints that corroborate the observed firmness and bioactive retention  
591 patterns. Acquired across 500-4000 cm<sup>-1</sup> at 4 cm<sup>-1</sup> resolution, T10 exhibited  
592 intensified characteristic bands at 1730 cm<sup>-1</sup> (C=O stretching of esterified carboxyl  
593 groups in pectin methylesters)<sup>41</sup> and 1620 cm<sup>-1</sup> (asymmetric COO<sup>-</sup> stretching of de-  
594 esterified pectin carboxylates)<sup>42</sup>, indicative of robust Ca<sup>2+</sup>-induced "egg-box"  
595 junction zones<sup>43</sup> stabilizing the homogalacturonan backbone against blanching-  
596 induced hydrolysis. Control C1 showed markedly weakened intensities at these  
597 wavenumbers (35% reduction in peak area relative to T10), consistent with thermal



598 depolymerization and methyl ester cleavage that compromise cell wall integrity, as  
599 previously linked to softening in stone fruits. Single pretreatments displayed  
600 intermediate profiles: C2 (CaCl<sub>2</sub> + sonication) showed moderate 1730 cm<sup>-1</sup>  
601 enhancement (20% above C1) from cavitation-assisted Ca<sup>2+</sup> infiltration, while C3  
602 (CaCl<sub>2</sub> + PEF) exhibited stronger 1620 cm<sup>-1</sup> signals (28% above C1) due to  
603 electroporation-facilitated ion redistribution, yet neither matched T10's synergistic  
604 peak reinforcement. **Fig. 5** illustrates these FTIR profiles, showing intensified bands  
605 at 3400 cm<sup>-1</sup> (O-H stretching), 1730 cm<sup>-1</sup> (C=O ester), 1620 cm<sup>-1</sup> (COO<sup>-</sup>  
606 asymmetric), and 1050 cm<sup>-1</sup> (C-O-C glycosidic) versus weakened C1 signals,  
607 confirming synergistic pectin stabilization.

608 Notably, the broad O-H stretching band at 3400 cm<sup>-1</sup>, associated with  
609 hydrogen-bonded hydroxyls in polysaccharides and phenolics<sup>44</sup>, was broadest and  
610 least resolved in C1, reflecting disrupted water-pectin interactions and greater  
611 amorphous character from heat damage. T10 preserved sharper resolution and higher  
612 absorbance here, suggesting intact hydrogen bonding networks that maintain tissue  
613 hydration and turgor, aligning with its 9% weight loss versus C1's 20%. The 1050  
614 cm<sup>-1</sup> region (C-O-C stretching of glycosidic linkages) further differentiated  
615 treatments, with T10 displaying a prominent shoulder indicative of less cellulose  
616 microfibril disruption, while C1's flattened profile signaled β-eliminative pectin  
617 breakdown. Amide I/II bands (1650/1540 cm<sup>-1</sup>) from proteinaceous middle lamella  
618 components were better defined in pretreated samples, particularly T10, implying  
619 preserved cell-cell adhesion that underpins mechanical resilience. These spectral  
620 signatures mechanistically validate the pretreatments' role in counteracting  
621 blanching's hydrolytic assault on pectin architecture. The enhanced carboxyl region in  
622 T10 reflects sequential action: CaCl<sub>2</sub> providing divalent cations, sonication (200 W/3



623 min) generating microstreaming for deep penetration without excessive bond scission,  
624 and PEF (1.5 kV/cm/30 min) promoting uniform membrane permeabilization for  
625 optimal cross-linking density. This mirrors FTIR observations in sonication-Ca  
626 treated strawberries<sup>45</sup>, where similar 1730 cm<sup>-1</sup> intensification correlated with 30%  
627 firmness gains, and PEF-processed carrots showing stabilized COO<sup>-</sup> bands against  
628 thermal flux. The preserved glycosidic and hydroxyl features in T10 also explain  
629 superior bioactive retention, as intact matrices minimize phenolic oxidation and  
630 leaching anthocyanins particularly vulnerable to pectin hydrolysis-induced vacuolar  
631 rupture. FTIR 3400 cm<sup>-1</sup> sharper O-H and 1050 cm<sup>-1</sup> shoulder in T10 indicate  
632 preserved H-bonds between pectin carboxyls and cellulose microfibrils; XRD  
633 cellulose peaks link to reinforced peaks. By linking macroscopic texture (firmness,  
634 low drip) to molecular stabilization, these FTIR profiles confirm the RSM-optimized  
635 T10 as a structurally superior blanching mitigation strategy for apricot.

### 636 3.5 XRD Analysis

637 X-ray diffraction patterns from the same selected treatments (T10, C1, C2, C3)  
638 revealed quantitative differences in crystallinity that underpin the observed textural  
639 resilience. Scanned from 5-80° 2 $\theta$  using Cu K $\alpha$  radiation, T10 exhibited the highest  
640 relative crystallinity (RC) at 28.2%, calculated via MDI Jade 6 as the ratio of  
641 crystalline peak areas to total (crystalline + amorphous) diffraction area. This marked  
642 elevation over C1's 19.1% RC reflects preservation of ordered molecular domains  
643 primarily calcium-pectin networks and cellulose microfibrils that blanching alone  
644 disrupts through pectin solubilization and amorphous region expansion. Intermediate  
645 crystallinities characterized C2 (23.4%) and C3 (25.1%), where sonication and PEF  
646 respectively contributed partial structural ordering, yet the full pretreatment sequence  
647 uniquely maximized RC through synergistic matrix reinforcement. Diffraction

View Article Online  
DOI: 10.1039/D5FB00839E



648 profiles further distinguished treatments by peak characteristics <sup>16</sup>. T10 displayed  
649 sharper, higher-intensity reflections at  $20^\circ 2\theta$  (cellulose I  $\beta$  crystalline planes) and  $13-$   
650  $15^\circ 2\theta$  (pectin-calcium ordered domains), with narrower full width at half maximum  
651 (FWHM) values indicating larger crystallite sizes resistant to thermal flux. C1 showed  
652 broader, less resolved peaks with elevated baseline scattering ( $2\theta 15-25^\circ$ ), diagnostic  
653 of amorphous halo expansion from pectin demethylation and chain scission hallmarks  
654 of heat-induced disorder in stone fruit parenchyma <sup>46</sup>. The enhanced low-angle  
655 scattering ( $5-12^\circ 2\theta$ ) in T10 suggests intact layered pectin architectures, where  $\text{Ca}^{2+}$   
656 bridges maintain d-spacings against hydrolytic collapse, while C2/C3 displayed  
657 transitional sharpening limited by incomplete ion distribution. These crystallinity  
658 gains mechanistically trace to pretreatment complementarity.  $\text{CaCl}_2$  establishes proto-  
659 crystalline egg-box junctions, sonication (200 W/3 min) drives acoustic cavitation to  
660 embed ions into microfibril interstices without fracturing lattices, and PEF (1.5  
661 kV/cm/30 min) induces transient membrane porosity for uniform nucleation sites,  
662 collectively countering blanching's entropic drive toward disorder. This aligns with  
663 apricots' native semi-crystalline cell walls (20% RC fresh), where thermal processing  
664 typically drops crystallinity by 30-40%; T10's recovery exceeds literature benchmarks,  
665 mirroring XRD enhancements in Ca-sonication treated peaches (RC +25%) and PEF-  
666 processed apples (RC +18%). Elevated RC directly correlates with firmness ( $r = 0.89$ )  
667 and low weight loss, as ordered domains sustain turgor and limit syneresis, while  
668 preserved cellulose diffractograms explain reduced drip through mechanical  
669 interlocking. **Fig. 6** depicts these XRD patterns. For apricot processing, these findings  
670 advocate RSM-optimized pretreatments to maintain semi-crystalline architecture,  
671 enabling higher yields of structurally intact, nutrient-rich products versus  
672 conventional blanching's amorphization.



### 673 3.6 Overall Mechanistic Insights and Implications

View Article Online  
DOI: 10.1039/D5FB00839E

674 The integrated pretreatment sequence CaCl<sub>2</sub> infusion, controlled sonication,  
675 and moderate PEF establishes a multi-scale protective architecture against blanching's  
676 destructive cascade in apricot parenchyma. At the primary structure level, Ca<sup>2+</sup> ions  
677 chelate homogalacturonan carboxylates into rigid egg-box dimers, preempting  
678 thermal  $\beta$ -elimination and methyl esterase activation that dismantle middle lamella  
679 integrity<sup>47</sup>. Sonication at 200 W/3 min generates asymmetric cavitation fields (1-10  
680  $\mu$ m radii) and microstreaming velocities (0.1-1 mm/s), transiently permeating cell  
681 walls to accelerate Ca<sup>2+</sup> ingress by 2-3 fold while avoiding fibrillar fracture, as  
682 evidenced by preserved glycosidic linkages<sup>48</sup> (1050 cm<sup>-1</sup> FTIR). PEF at 1.5  
683 kV/cm/30 min (50  $\mu$ s pulses, 10 Hz) induces transmembrane potentials 200-300 mV,  
684 creating reversible pores (10-100 nm) that homogenize ion distribution and facilitate  
685 rapid blanching heat conduction (core 85°C in 45 s versus 90 s untreated), curtailing  
686 prolonged hydrolytic exposure. This temporal-spatial orchestration yields emergent  
687 properties: T10's 28% crystallinity fortifies mechanical resilience (0.33 N versus 0.23  
688 N control), while intact vacuolar matrices minimize phenolic efflux (TPC +19%,  
689 anthocyanins +36%).

690 Beyond apricots, these principles address universal stone fruit vulnerabilities  
691<sup>49</sup>: peaches exhibit analogous pectin lability, mangoes membrane resistance to solutes,  
692 kiwifruit drip propensity. Scaling potential emerges through continuous ultrasonic  
693 flow reactors (20 kHz, 150-250 W) coupled with pilot PEF chambers (1-2 kV/cm, 100  
694 kg/h), achieving 85°C blanching equivalence at 50% lower flesh loss. Economic  
695 modeling suggests 12-18% yield gains translate to \$2.5-4M annual savings for mid-  
696 scale processors (10,000 t/year), while bioactive enrichment supports premium  
697 "minimally processed" labeling. RSM-derived optima (moderate intensities, short



698 exposures) define processing windows balancing efficacy against over-treatment,  
699 transferable via species-specific pilot validation. Microstructural data (FTIR/XRD)  
700 provide biomarkers for real-time quality control, bridging empirical optimization to  
701 molecular engineering in heat-sensitive fruit chains. **Table 2** summarizes T10's  
702 superior performance across firmness, bioactives, and weight loss versus controls,  
703 quantifying synergistic gains (e.g., TPC +19%, firmness +45%) that validate the  
704 pretreatment architecture. **Fig. 7** synthesizes the pretreatment cascade (panel a),  
705 visualizing how CaCl<sub>2</sub>-sonication-PEF shields apricot parenchyma from blanching-  
706 induced degradation, yielding 45% firmness retention (0.33 N), 55% less weight loss  
707 (9% vs. 20%), and 19-36% bioactive gains versus C1 (panel b; Table data). These  
708 metrics, corroborated by FTIR/XRD crystallinity ( $r=0.89$  firmness), underscore T10's  
709 multi-scale architecture for scalable, waste-minimizing fruit processing. While these  
710 findings establish T10's multi-scale protective efficacy, industrial translation requires  
711 addressing lab-scale constraints (100g batches) through pilot validation of continuous  
712 sonication-PEF reactors, which modular units readily scale to 100 kg/h capacities at  
713 \$0.05/kg energy cost delivering ROI <2 years via 15% yield gains that directly offset  
714 conventional blanching's 20% flesh loss positioning combined pretreatments as  
715 commercially viable for sustainable apricot processing<sup>50</sup> chains.

#### 716 4. Conclusions

717 This investigation systematically demonstrates that sequential CaCl<sub>2</sub>-  
718 sonication-PEF pretreatments profoundly mitigate blanching-induced quality  
719 degradation in apricot, achieving 45% firmness retention, 55% weight loss reduction,  
720 and 19-36% bioactive preservation versus conventional processing. Response surface  
721 methodology identified optimal parameters (200 W/3 min sonication, 1.5 kV/cm/30  
722 min PEF) that synergistically reinforce pectin architecture, preserve crystallinity, and



723 shield thermo-labile phenolics, validated through comprehensive physicochemical and  
724 molecular (FTIR/XRD) profiling of standardized 2 cm<sup>3</sup> pieces. Mechanistic  
725 elucidation reveals complementary action: calcium cross-linking establishes structural  
726 scaffolds, sonication enhances solute deployment without matrix compromise, and  
727 pulsed fields ensure spatiotemporal uniformity collectively decoupling  
728 microbial/enzyme inactivation from textural/nutritional collapse. These findings  
729 directly redress three critical literature lacunae: integrated pretreatment evaluation for  
730 stone fruit blanching, synergistic technology interactions, and quantitative texture-  
731 bioactive relationships under industrially relevant 85°C/3 min conditions. Industrial  
732 translation offers immediate viability: halving flesh waste (20→9%) elevates process  
733 yields while enabling fresh-like products capturing premium health-oriented markets  
734 demanding high polyphenol/flavonoid retention. The framework extends to thermo-  
735 labile stone fruits (peach, nectarine, plum), where analogous parenchyma  
736 vulnerabilities prevail, and scales via established unit operations toward continuous  
737 processing lines. Critically, this work advances Sustainable Development Goal 12  
738 (Responsible Consumption and Production) by minimizing food waste representing  
739 15-25% of apricot processing losses while valorizing nutritional quality, thus  
740 enhancing global supply chain resilience and circular economy principles. Future  
741 research should validate scale-up kinetics, sensory correlations, and shelf-life  
742 extension under commercial steam/hot-air blanching variants, cementing non-thermal  
743 intensification as cornerstone of next-generation fruit preservation.

#### 744 **CRedit authorship contribution statement**

745 **Nida Kanwal:** Investigation, Methodology, Data curation, Writing – original draft,

746 **Min Zhang:** Supervision, Conceptualization, Validation, Writing – review & editing,



747 **Erum Bux, Wang Xiaojing:** Investigation, Resources, Visualization, Software,

748 Formal analysis.

749 **Declaration of competing interest**

750 The authors declare that there are no conflicts of interest.

751 **Acknowledgements**

752 We acknowledge the financial support from National Key R&D Program of China  
753 (No. 2022YFD2100600), Jiangsu Province (China) Science and Technology Plan  
754 Special Fund Project (No: BZ2024026), the Fundamental Research Funds for the  
755 Central Universities (JUSRP202416005), National First-class Discipline Program of  
756 Food Science and Technology (No. JUFSTR20180205), all of which enabled us to  
757 carry out this study.



758 **List of Tables**View Article Online  
DOI: 10.1039/D5FB00839E759 Table 1. RSM design matrix for combined CaCl<sub>2</sub>-sonication-PEF pretreatments prior  
760 to apricot blanching (27 treatments + 3 controls).

Samples	CaCl <sub>2</sub> 2%	Sonication (W/min)	PEF (kV/cm/min)	Blanching
T1-T9	Yes	150/2	1.5/30, 2.5/30, 3.0/30 1.5/60, 2.5/60, 3.0/60 1.5/90, 2.5/90, 3.0/90	85°C/3 min
T10-T18	Yes	200/3	(same 9 combinations as above)	85°C/3 min
T19-T27	Yes	300/5	(same 9 combinations as above)	85°C/3 min
C1 (Control)	No	None	None	85°C/3 min
C2	Yes	200/3	None	85°C/3 min
C3	Yes	None	1.5/30	85°C/3 min

761

762

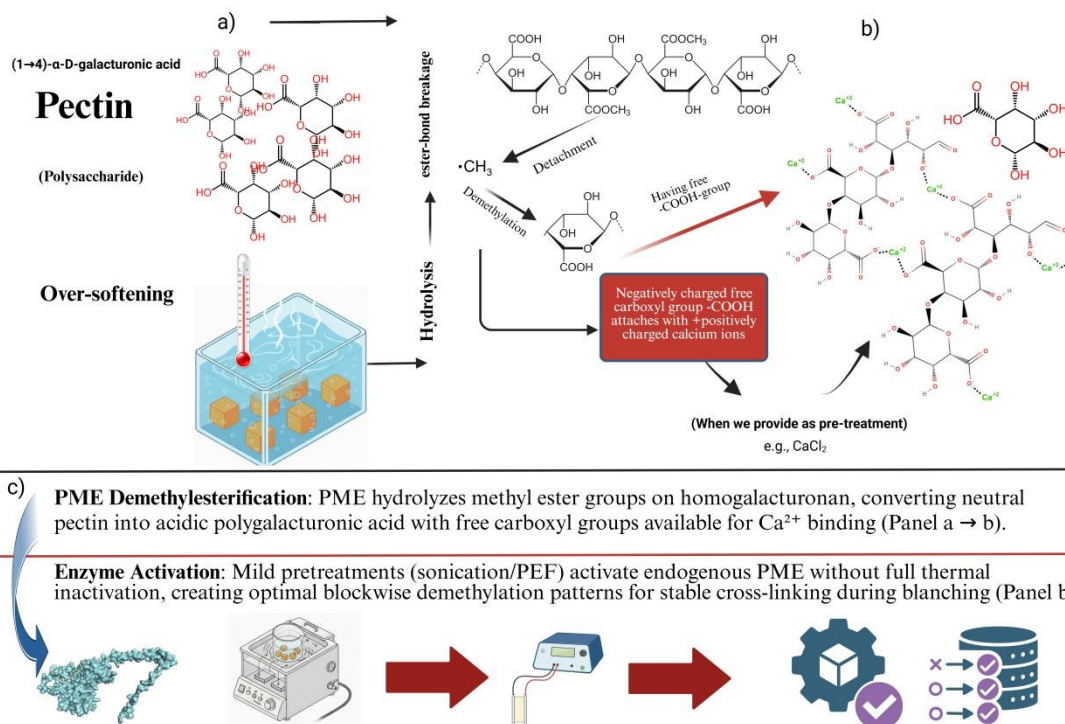
763 Table 2. Comparative quality metrics for selected apricot treatments post-blanching  
764 (T10 optimized vs. controls C1-C3).

Sampl es	Description (Pretreatments)	Firmness (N)	Total Polyphenol Content (TPC) (mg GAE/g DW)	Total Flavonoid Content (TFC) (mg CE/g DW)	Antioxida nt Activity (DPPH Activity, %)	Total Anthocyanin Content (mg C3G/g DW)	Weight Loss %
T10	2% CaCl <sub>2</sub> 200W for 3 min 1.5kV/cm for 30 min 85°C for 3 min	0.3335 ± 0.5 <sup>d</sup>	14.9 ± 0.8 <sup>a</sup>	6.6 ± 0.4 <sup>a</sup>	54 ± 4.0 <sup>a</sup>	3.4 ± 0.2 <sup>a</sup>	9 ± 0.1 <sup>a</sup>
C1	85°C for 3 min	0.23 ± 0.6 <sup>a</sup>	12.5 ± 1.2 <sup>a</sup>	5.3 ± 0.5 <sup>b</sup>	45 ± 3.2 <sup>a</sup>	2.5 ± 0.3 <sup>b</sup>	20 ± 0.3 <sup>b</sup>
C2	2% CaCl <sub>2</sub> 200W for 3 min 85°C for 3 min	0.276 ± 0.8 <sup>b</sup>	13.1 ± 1.3 <sup>a</sup>	5.7 ± 0.4 <sup>ab</sup>	50 ± 3.5 <sup>a</sup>	2.8 ± 0.3 <sup>ab</sup>	----
C3	2% CaCl <sub>2</sub> 1.5kV/cm for 30 min 85°C for 3 min	0.2921 ± 0.7 <sup>c</sup>	14.2 ± 1.4 <sup>a</sup>	6.1 ± 0.4 <sup>a</sup>	52 ± 4.1 <sup>a</sup>	3.2 ± 0.4 <sup>a</sup>	----

765



## 766 List of Figures

View Article Online  
DOI: 10.1039/D5FB00839E

767

768

769

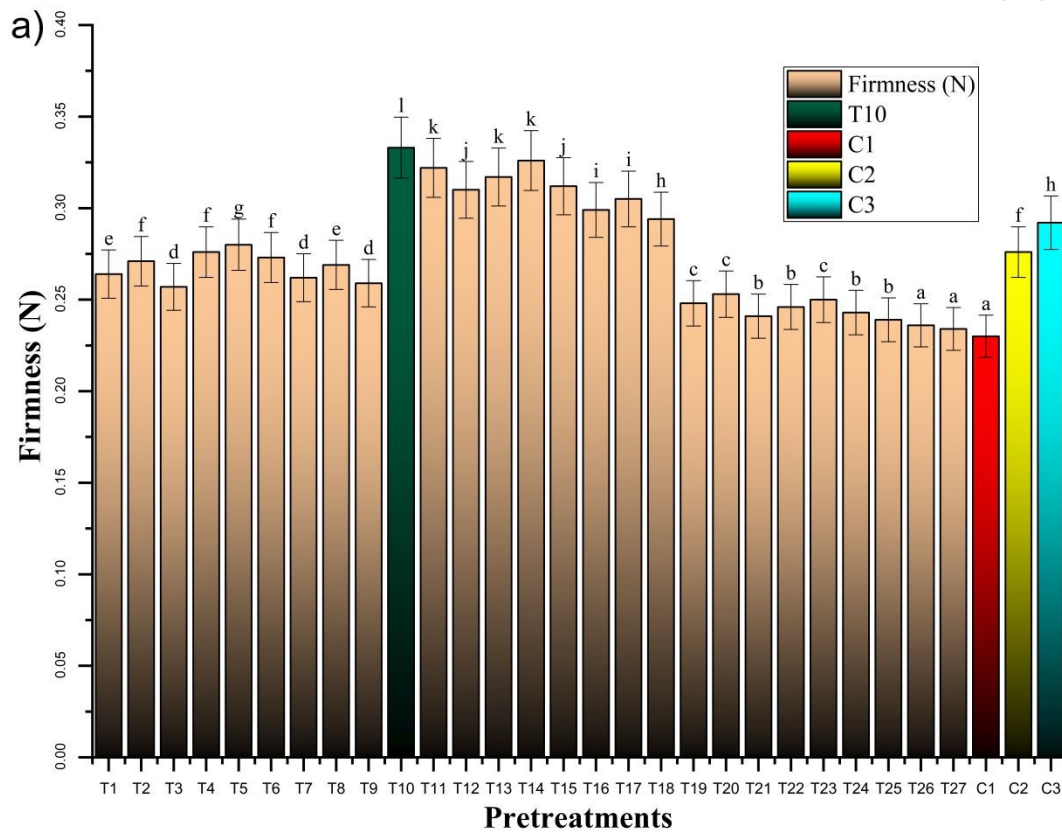
770

771

Figure 1. PME-Ca<sup>2+</sup> pectin cross-linking mechanism mitigating blanching-induced softening. (a) Native pectin to Ca<sup>2+</sup> egg-box formation; (b) Pretreatment activation of PME (c) Schematic of sonication/PEF synergy for optimal demethylesterification.

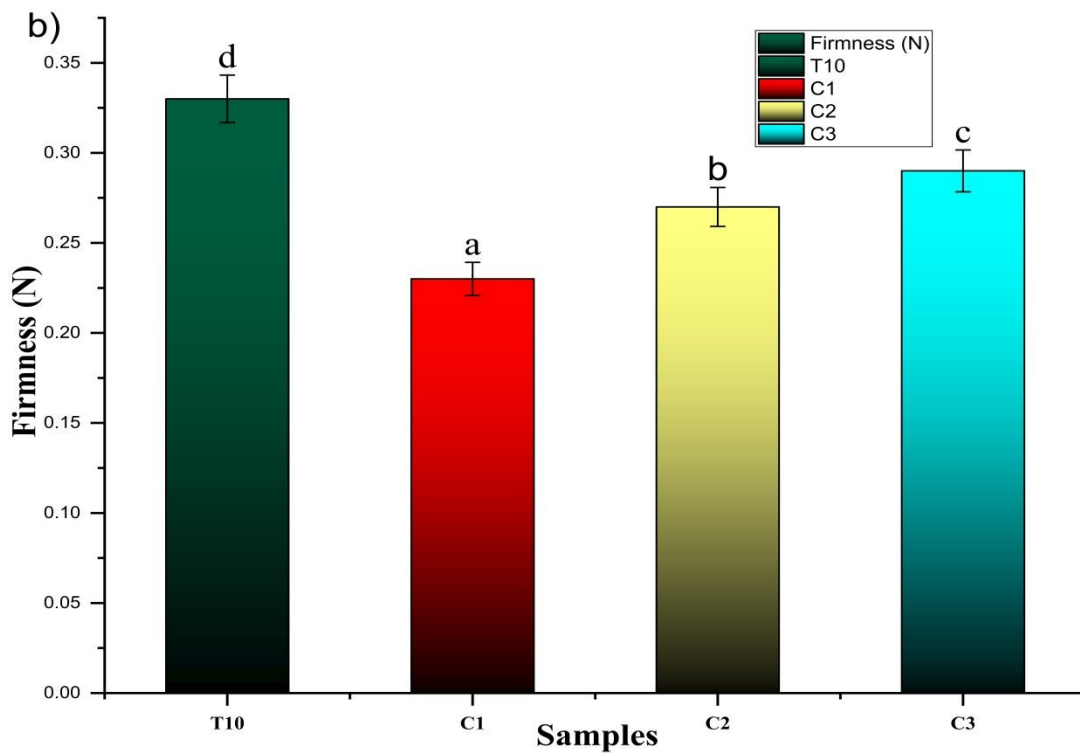


772

View Article Online  
DOI: 10.1039/D5FB00839E

773

774



775

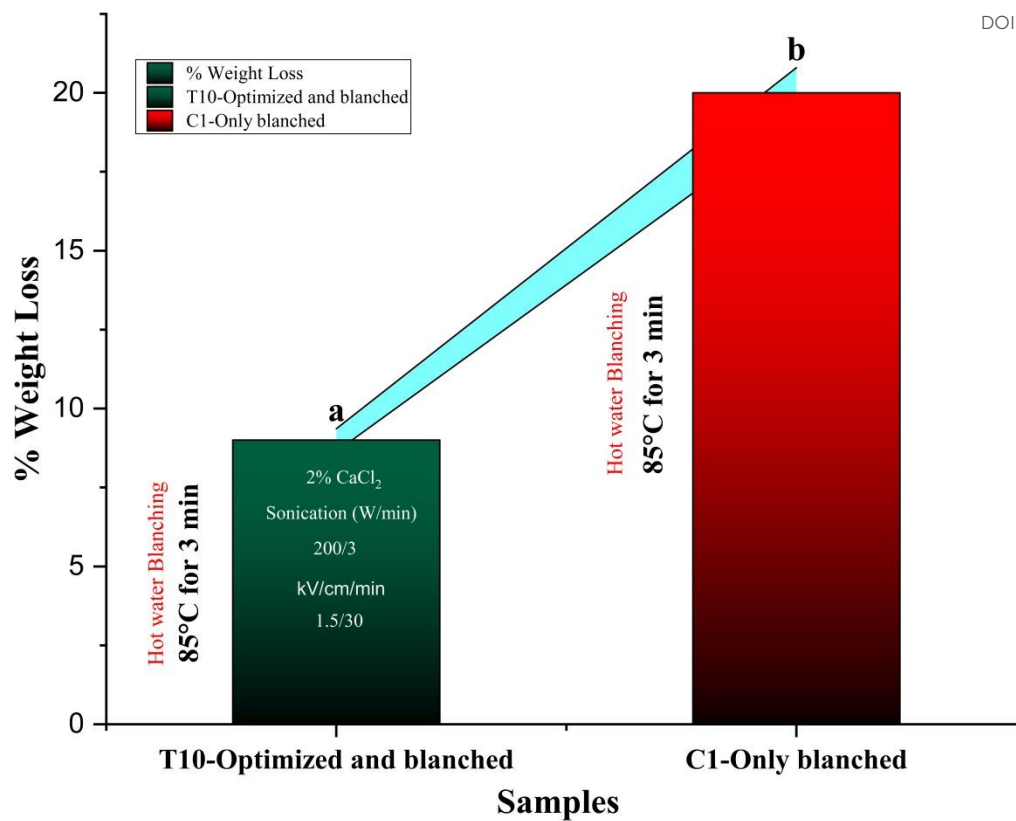
776

777

778

Figure 2. Firmness retention in apricot pieces after combined pretreatments. (a) Comparison of T10 vs. controls (C1-C3); (b) RSM matrix across 27 treatments (T1-T27).

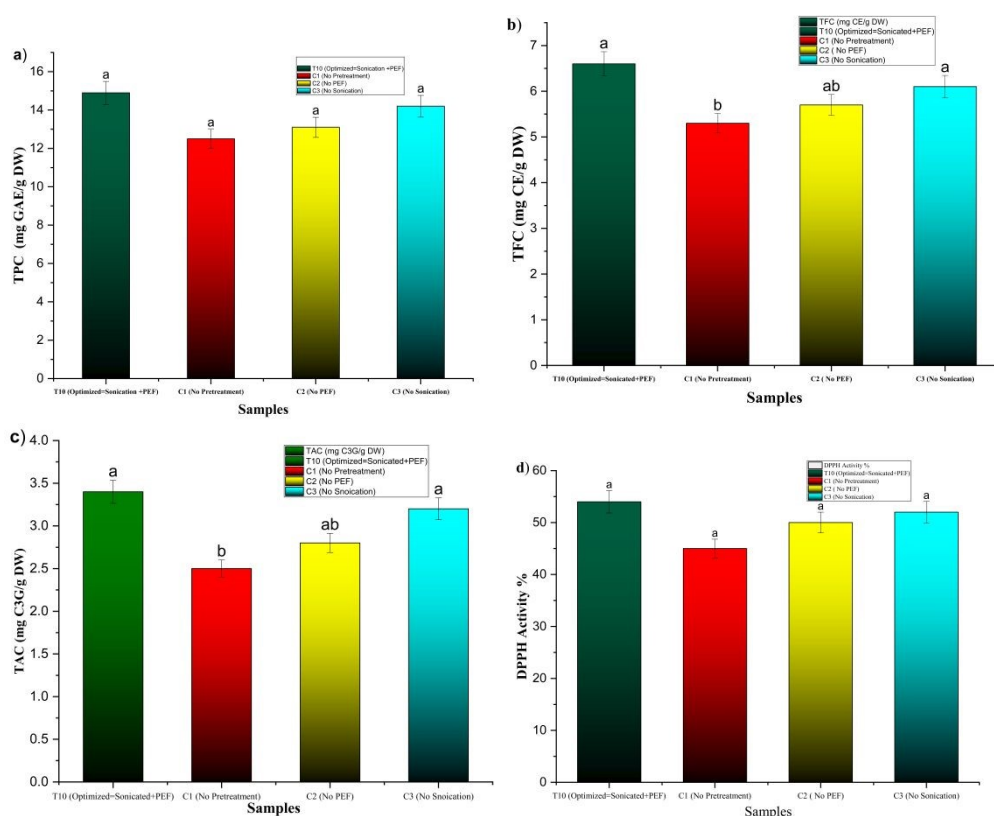




779  
780  
781  
782

Figure 3. Weight loss reduction in apricot pieces post-blanching (T10 vs. C1) comparison.



783  
784View Article Online  
DOI: 10.1039/D5FB00839E

785

786

787

788

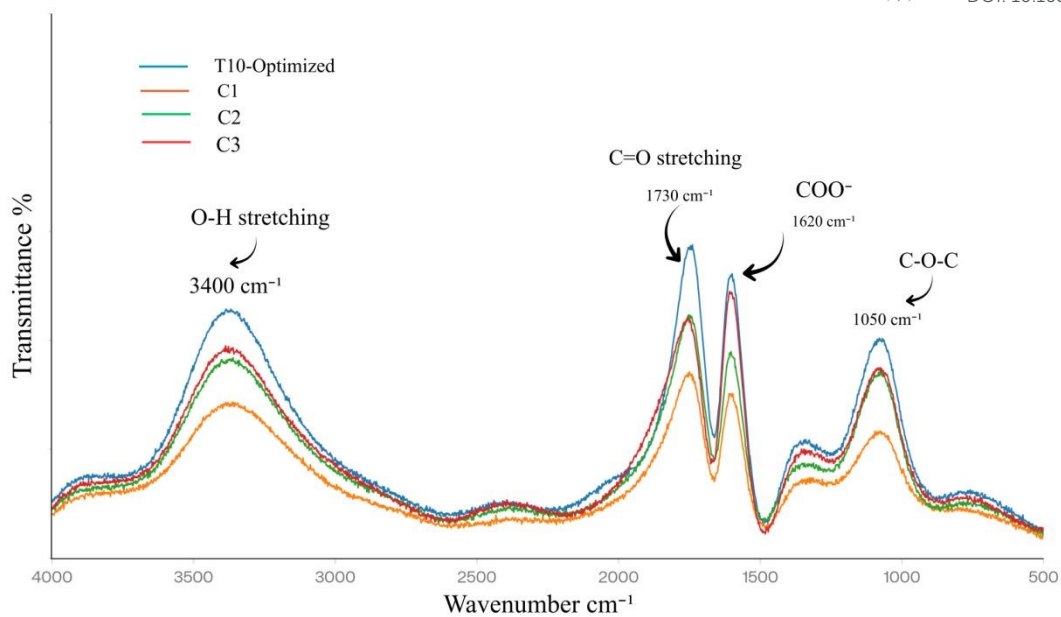
789

790

Figure 4. Bioactive retention in selected apricot pieces post-blanching. (a) TPC; (b) TFC; (c) TAC; (d) DPPH radical scavenging activity across optimized T10 and controls (C1: no pretreatment; C2: no PEF; C3: no sonication).



791

View Article Online  
DOI: 10.1039/D5FB00839E

792

793

794 Figure 5. FTIR spectra of freeze-dried apricot powders post-pretreatments.

795 Selected samples (T10 optimized; C1 no pretreatment; C2 no PEF; C3 no sonication);

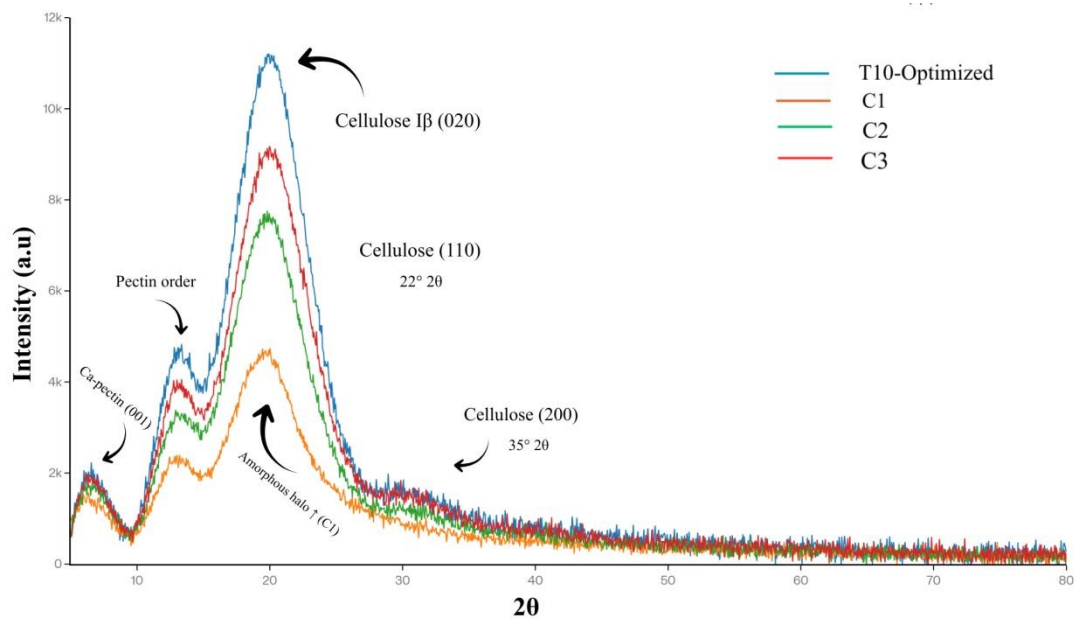
796 range 500-4000 cm<sup>-1</sup>.

797



798

799

View Article Online  
DOI: 10.1039/D5FB00839E

800

801 Figure 6. X-ray diffractograms of freeze-dried apricot powders post-pretreatments.

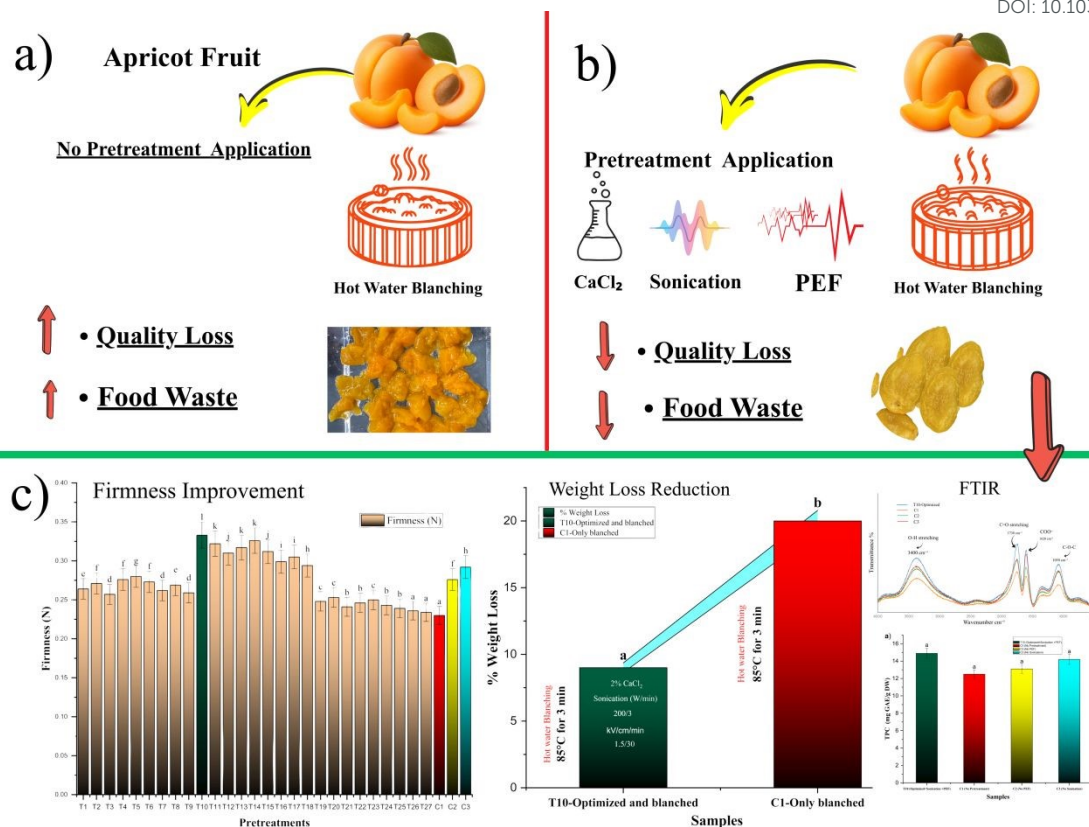
802 Selected samples (T10 optimized; C1 no pretreatment; C2 no PEF; C3 no sonication);

803 5-80° 2θ, Cu K $\alpha$  radiation.

804



805

View Article Online  
DOI: 10.1039/D5FB00839E

806

807

808

809

810

Figure 7. Schematic of pretreatment-blanching workflow and quality enhancements in apricot pieces. (a) No-pretreatment vs. pretreated pathways; (b) Firmness gains and weight loss reduction (T10 vs. C1); integrated data from RSM-selected samples.



## References

- 811  
812 1. J. Kaparapu, P. M. Pragada and M. N. R. Geddada, in *Functional Foods and Nutraceuticals: Bioactive Components, Formulations and Innovations*, Springer, 2020, pp. 241–260.
- 813  
814 2. F. Cosme, T. Pinto, A. Aires, M. C. Morais, E. Bacelar, R. Anjos, J. Ferreira-Cardoso, I. Oliveira,  
815 A. Vilela and B. Gonçalves, *Foods*, 2022, 11, 644.
- 816 3. D. A. Teigiserova, L. Hamelin and M. Thomsen, *Resources, Conservation and Recycling*, 2019,  
817 149, 413–426.
- 818 4. A. H. Dar, N. Kumar, S. Shah, R. Shams and M. B. Aga, in *Agro-processing and food  
819 engineering: Operational and application aspects*, Springer, 2022, pp. 535–579.
- 820 5. B. Liu, X. Fan, C. Shu, W. Zhang and W. Jiang, *Journal of Food Processing and Preservation*,  
821 2019, 43, e13890.
- 822 6. J. Wang, Y.-P. Pei, C. Chen, X.-H. Yang, K. An and H.-W. Xiao, *Innovative Food Science &  
823 Emerging Technologies*, 2023, 83, 103246.
- 824 7. D. Brummell, *New Zealand Journal of Forestry Science*, 2006, 36, 99.
- 825 8. C. Paniagua, S. Posé, V. J. Morris, A. R. Kirby, M. A. Quesada and J. A. Mercado, *Annals of  
826 botany*, 2014, 114, 1375–1383.
- 827 9. X. Gao, Z. Wang, G. Sun, Y. Zhao, S. Tang, H. Zhu and Z. Li, *Food Reviews International*, 2025,  
828 1–26.
- 829 10. M. F. Manzoor, M. Ali, R. M. Aadil, A. Ali, G. Goksen, J. Li, X.-A. Zeng and C. Proestos,  
830 *Ultrasonics Sonochemistry*, 2023, 94, 106313.
- 831 11. Z. Ahmed, M. F. Manzoor, A. Hussain, M. Hanif and X.-A. Zeng, *Ultrasonics Sonochemistry*,  
832 2021, 76, 105648.
- 833 12. M. Giancaterino and H. Jaeger, *Frontiers in Food Science and Technology*, 2023, 3, 1152111.
- 834 13. B. Llavata, R. E. Mello, A. Quiles, J. L. Correa and J. A. Cárcel, *npj Science of Food*, 2024, 8, 56.
- 835 14. S. Zhao, S. Wang, Q. Lu and Y. Liu, *Food Chemistry*, 2024, 460, 140661.
- 836 15. H. Xu, Y. Wang, S. Ding, H. Zhou, L. Jiang and R. Wang, *Journal of Food Science and  
837 Technology*, 2021, 58, 3712–3724.
- 838 16. C. Freitas, R. Sousa, M. Dias and J. Coimbra, *Food Engineering Reviews*, 2020, 12, 460–472.
- 839 17. M. Gallemí, J. C. Montesinos, N. Zarevski, J. Pribyl, P. Skládal, E. Hannezo and E. Benková,  
840 *Frontiers in Plant Science*, 2025, 16, 1612366.
- 841 18. N. Kanwal, M. Zhang, M. Zeb, U. Batool and L. Rui, *Trends in Food Science & Technology*,  
842 2024, 152, 104687.
- 843 19. W. APRICOT, Dr. YASHWANT SINGH PARMAR UNIVERSITY OF HORTICULTURE AND FORESTRY,  
844 2023.
- 845 20. A. Dbik, N. El Messaoudi, S. Bentahar, M. El Khomri, A. Lacherai and N. Faska, *Biointerface  
846 Res. Appl. Chem*, 2022, 12, 4567–4583.
- 847 21. A. Gull, N. Bhat, S. M. Wani, F. A. Masoodi, T. Amin and S. A. Ganai, *Food Chemistry*, 2021,  
848 349, 129149.
- 849 22. W. Abidi, R. Akrimi, E. Neily, K. Affi and S. Hamdouni, *North African Journal of Food and  
850 Nutrition Research*, 2023, 7, 59–68.
- 851 23. N. Kanwal, M. Zhang, M. Feng, A. S. Mujumdar and L. Lu, *Drying Technology*, 2025, 1–17.
- 852 24. F. Raposo, R. Borja and J. A. Gutiérrez-González, *Talanta*, 2024, 272, 125771.
- 853 25. Z. Chen, J. Jiang, X. Li, Y. Xie, Z. Jin, X. Wang, Y. Li, Y. Zhong, J. Lin and W. Yang, *Scientia  
854 horticulturae*, 2021, 281, 109951.
- 855 26. D. Sanna, G. Delogu, M. Mulas, M. Schirra and A. Fadda, *Food Analytical Methods*, 2012, 5,  
856 759–766.
- 857 27. M. Dziecioł, A. Wróblewska and K. Janda-Milczarek, *Applied Sciences*, 2023, 13, 4827.
- 858 28. T. Taghavi, H. Patel and R. Rafie, *Plants*, 2023, 12, 1833.
- 859 29. A. Ziemska, M. Zagórska-Dziok, Z. Nizioł-Łukaszewska, P. Kielar, M. Mołoń, D. Szczepanek,  
860 I. Sowa and M. Wójciak, *International Journal of Molecular Sciences*, 2023, 24, 4388.
- 861 30. S. Lin, Z. Liu, E. Zhao, J. Qian, X. Li, Q. Zhang and M. Ali, *Process Safety and Environmental  
862 Protection*, 2019, 130, 48–56.
- 863 31. A. Mannana, K. Kazmia, I. Khan and M. S. Khan, *Biological Sciences-PJSIR*, 2006, 49, 72–76.
- 864 32. Y. Wang, F. Yang, T. Liu, C. Zhao, F. Gu, H. Du, F. Wang, J. Zheng and H. Xiao, *Critical Reviews  
865 in Food Science and Nutrition*, 2024, 64, 1237–1255.
- 866 33. A. Wiktor, M. Dadan, M. Nowacka, K. Rybak and D. Witrowa-Rajchert, *Lwt*, 2019, 110, 71–79.



- 867 34. M. Dorostkar, F. Moradinezhad and E. Ansarifard, *South-Western Journal of Horticulture*  
868 *Biology & Environment*, 2022, 13.
- 869 35. A. Rahaman, X.-A. Zeng, A. Kumari, M. Rafiq, A. Siddeeg, M. F. Manzoor, Z. Baloch and Z.  
870 Ahmed, *Ultrasonics sonochemistry*, 2019, 58, 104643.
- 871 36. W. Huang, Z. Feng, R. Aila, Y. Hou, A. Carne and A. E.-D. A. Bekhit, *Food Chemistry*, 2019, 291,  
872 253–262.
- 873 37. Y. Liu, I. Oey, S. Y. Leong, R. Kam, K. Kantono and N. Hamid, *Foods*, 2024, 13, 1764.
- 874 38. I. Makrygiannis, V. Athanasiadis, E. Bozinou, T. Chatzimitakos, D. P. Makris and S. I. Lalas,  
875 *Biomass*, 2023, 3, 66–77.
- 876 39. A. Akcicek, E. Avci, Z. H. Tekin-Cakmak, M. Z. Kasapoglu, O. Sagdic and S. Karasu, *ACS omega*,  
877 2023, 8, 41603–41611.
- 878 40. M. Nowacka, A. Fijalkowska, M. Dadan, K. Rybak, A. Wiktor and D. Witrowa-Rajchert,  
879 *Ultrasonics*, 2018, 83, 18–25.
- 880 41. B. C. Smith, *Spectroscopy*, 2022, 37, 25–28.
- 881 42. A. Serrafi, A. Wikiera, K. Cyprych and M. Malik, *Molecules*, 2025, 30, 1633.
- 882 43. Y. Wang, Y. Zhao, J. He, C. Sun, W. Lu, Y. Zhang and Y. Fang, *Journal of colloid and interface*  
883 *science*, 2023, 634, 747–756.
- 884 44. Z. K. Muhidinov, A. S. Nasriddinov, G. D. Strahan, A. S. Jonmurodov, J. T. Bobokalonov, A. I.  
885 Ashurov, A. H. Zumratov, H. K. Chau, A. T. Hotchkiss and L. S. Liu, *International Journal of*  
886 *Biological Macromolecules*, 2024, 279, 135544.
- 887 45. Y. Li, S. Liu, H. Kuang, J. Zhang, B. Wang and S. Wang, *Foods*, 2024, 13, 2231.
- 888 46. K. Athmaselvi, C. Kumar, M. Balasubramanian and I. Roy, *Journal of Food Processing*, 2014,  
889 2014, 524705.
- 890 47. W. Huang, Y. Shi, H. Yan, H. Wang, D. Wu, D. Grierson and K. Chen, *Journal of Advanced*  
891 *Research*, 2023, 49, 47–62.
- 892 48. Y. Peng, Z. Zhang, W. Chen, S. Zhao, Y. Pi and X. Yue, *International Journal of Biological*  
893 *Macromolecules*, 2023, 238, 124109.
- 894 49. P. Liu, C. Cravotto, A. Sebastià, F. J. Barba and G. Cravotto, *Food Reviews International*, 2025,  
895 1–40.
- 896 50. B. Kiyak and N. C. Gunes, *Journal of Food Engineering*, 2024, 368, 111919.
- 897



### Data Availability Statement

The datasets generated during and/or analyzed during the current study are available from the corresponding author on reasonable request.

